Article

A Red Algal Bourbonane Sesquiterpene Synthase Defined by Microgram-scale NMR-coupled Crystalline Sponge XRD Analysis

Roland D. Kersten, Shoukou Lee, Daishi Fujita, Tomáš Pluskal, Susan Kram, Jennifer E. Smith, Takahiro Iwai, Joseph P. Noel, Makoto Fujita, and Jing-Ke Weng

J. Am. Chem. Soc., **Just Accepted Manuscript** • DOI: 10.1021/jacs.7b09452 • Publication Date (Web): 30 Oct 2017

A Red Algal Bourbonane Sesquiterpene Synthase Defined by Microgram-scale NMR-coupled Crystalline Sponge XRD Analysis

Roland D. Kersten[1,#], Shoukou Lee[2,#], Daishi Fujita[1,2], Tomáš Pluskal[1], Susan Kram[3], Jennifer E. Smith[3], Takahiro Iwai[2], Joseph P. Noel[4], Makoto Fujita[2,*], Jing-Ke Weng[1,5,*]

1 - Whitehead Institute for Biomedical Research, 455 Main Street, Cambridge, MA, United States
2 - Graduate School of Engineering, The University of Tokyo, JST-ACCEL, Tokyo, Japan
3 - Scripps Institution of Oceanography, University of California San Diego, La Jolla, CA, United States
4 - Howard Hughes Medical Institute, Jack H. Skirball Center for Chemical Biology and Proteomics, The Salk Institute for Biological Studies, La Jolla, CA, United States
5 – Department of Biology, Massachusetts Institute of Technology, Cambridge, MA, United States
# - these authors contributed equally
* - corresponding authors: mfujita@appchem.t.u-tokyo.ac.jp and wengj@wi.mit.edu

Supporting Information Placeholder

ABSTRACT: Sesquiterpene scaffolds are the core backbones of many medicinally and industrially important natural products. A plethora of sesquiterpene synthases, widely present in bacteria, fungi, and plants, catalyze the formation of these intricate structures often with multiple stereocenters starting from linear farnesyl diphosphate (FPP) substrates. Recent advances in next-generation sequencing and metabolomics technologies have greatly facilitated gene discovery for sesquiterpene synthases. However, a major bottleneck limits biochemical characterization of recombinant sesquiterpene synthases: the absolute structural elucidation of the derived sesquiterpene products. Here, we report the identification and biochemical characterization of LphTPS-A, a sesquiterpene synthase from the red macroalga *Laurencia pacifica*. Using the combination of transcriptomics, sesquiterpene synthase expression in yeast, and microgram-scale NMR-coupled crystalline sponge X-ray diffraction (XRD) analysis, we resolved the absolute stereochemistry of prespatane, the major sesquiterpene product of LphTPS-A, and thereby functionally define LphTPS-A as the first bourbonane-producing sesquiterpene synthase and the first biochemically characterized sesquiterpene synthase from red algae. Our study showcases a workflow integrating multi-omics approaches, synthetic biology, and the crystalline sponge method, which is generally applicable for uncovering new terpene chemistry and biochemistry from source-limited living organisms.

INTRODUCTION

Sesquiterpenes are ecologically, commercially, and medicinally important natural products produced by organisms from all domains of life.[1,2] Sesquiterpenes typically incorporate multicyclic hydrocarbon cores with several stereocenters. The core structures are generally biosynthesized by type I sesquiterpene synthases from linear farnesyl diphosphate (FPP) precursors, which can exist in several olefinic stereoisomers.[3] Efficient total synthesis of sesquiterpenes with stereocontrol in large amounts is often difficult;[4] therefore, identification of specific sesquiterpene synthases followed by metabolic engineering and semisynthesis is an important route for sustainable production of high-value sesquiterpene products.[5]

The rapid expansion of genomic resources available for non-model organisms has revealed tremendous sequence diversity of sesquiterpene synthase families in bacteria,[6] fungi,[7] plants,[8] and other eukaryotes,[9] underlying largely untapped natural sesquiterpene chemistry. While the number of biochemically characterized sesquiterpene synthases continues to increase, prediction of sesquiterpene synthase products solely based on primary sequence remains impractical.[10] Currently, reconstitution of sesquiterpene synthase activity in heterologous systems is an essential first step for sesquiterpene synthase characterization, which has been greatly expedited by recent advances in gene synthesis and metabolic engineering techniques in microbial hosts.[11,12] Gas chromatography–mass spectrometry (GC-MS) and nuclear magnetic resonance (NMR) are routinely used in combination to infer the structure of a given sesquiterpene, when sufficient amount of pure product can be obtained.[11,13] Additionally, NOESY NMR is often used to infer relative stereochemistry, but lacks the clarity needed to assign absolute stereochemistry. With these limitations, the absolute configuration of many previously reported sesquiterpenes has yet to be unequivocally demonstrated.

X-ray crystallography (Bijvoet method) is a well-established, direct method for absolute structure determination of small molecules. However, most sesquiterpenes exist as oil and are recalcitrant to crystallization. For those that do crystallize, anomalous X-ray scattering is often weak due to the lack of anomalously scattering atoms in sesquiterpenes, rendering significant difficulties for Bijvoet analysis.

The crystalline sponge method has recently emerged as a new methodology for structure elucidation of small organic molecules at microgram-to-nanogram scale.[14,15] The analyte, also referred to as the guest, is soaked into the pre-prepared crystals of porous metal-organic coordination complexes. The absorbed guests often adopt defined poses in the pores, and their absolute three-dimensional structure can then be determined by X-ray diffraction (XRD) analyses. The crystalline sponge method has been applied to resolve the absolute configuration of a wide array of terpenoids, including sesquiterpene oxidation products,[16] diterpene-derived plant hormones,[17] a fungal sesterterpene synthase product,[18] and marine sesquiterpene natural productss.[19] Here, we report the utility of the crystalline sponge method in the characterization of the first sesquiterpene synthase from a red macroalga by applying it for *de novo* structure elucidation of an unknown analyte in combination with NMR analysis.

RESULTS AND DISCUSSION

Marine organisms such as macroalgae are a prolific source of terpene-derived natural products.[20] In particular, red macroalgae under the family *Rhodomelaceae* produce a diversity of sesquiterpene natural products, many of which contain halogens and exhibit a multitude of unique bioactivities.[20] Of particular interest in red

macroalgal sesquiterpenes are their cyclic sesquiterpene scaffolds, which are often structurally distinct to scaffolds in sesquiterpenes from terrestrial sources.[20] Biosynthesis of red algal sesquiterpene scaffolds is hypothesized to involve two cyclization steps catalyzed by (a) sesquiterpene synthases and (b) vanadium-dependent bromoperoxidases.[20,21] While vanadium-dependent bromoperoxidases have been biochemically characterized as terpene cyclases in red macroalgae,[21] biochemical characterization of sesquiterpene synthase from red alga is still missing.

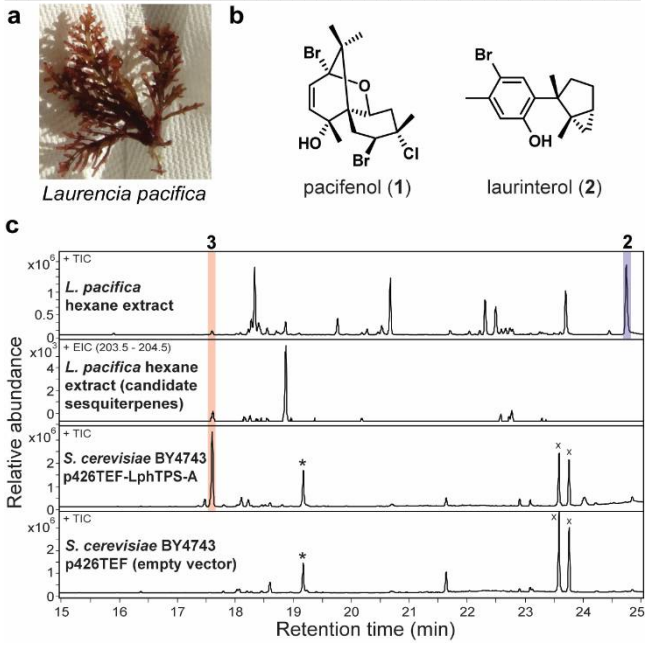

Figure 1. Terpene chemotyping of *Laurencia pacifica* and expression of LphTPS-A in yeast. (a) *L. pacifica* specimen. (b) Pacifenol (**1**) and laurinterol (**2**). (c) GC-MS detection of a candidate sesquiterpene (**3**) in *L. pacifica* hexane extract and reconstitution of the production of **3** in yeast by recombinant expression of LphTPS-A. The red bar highlights sesquiterpene **3**, the blue bar highlights laurinterol (**2**). Asterisk denotes (*E*,*E*)-farnesol and x denotes fatty acids based on NIST EI-MS match.

We targeted the red macroalga *Laurencia pacifica* (Figure 1a) for identification of sesquiterpene synthases catalyzing the hypothetical first committed step in sesquiterpene biosynthesis in these organisms, because several halogenated chamigrene and laurane sesquiterpenes have been identified from this species.[22] A specimen of *L. pacifica* was collected from La Jolla, CA, USA, and subjected to metabolic profiling by GC-MS. Pacifenol (**1**) and laurinterol (**2**) were detected in this specimen (Figure 1b, S1 & S2, Table S1 & S2). Additionally, several putative sesquiterpenes with the molecular formula $C_{15}H_{24}$ were also detected (Figure 1c). GC-MS analysis of these major sesquiterpene hydrocarbons yielded no high-scoring match to the deposited sesquiterpene spectra in the NIST database. These sesquiterpenes could either be putative biosynthetic precursors of pacifenol and laurinterol, or other sesquiterpene natural products produced by the alga or its associated microbiome.

To uncover the genetic and biochemical basis for the observed terpene chemotypes, we first performed RNA-Seq experiments using total RNA extracted from the combined tissue of a *L. pacifica* holobiont and assembled a *de novo* transcriptome using the Trinity assembler. Mining of the transcriptome identified three candidate sesquiterpene synthases, designated LphTPS-A, LphTPS-B, and LphTPS-C (Lph – *Laurencia pacifica* holobiont). Blast searches against GenBank revealed that LphTPS-A, -B, and -C are related to a number of predicted sesquiterpene synthases from cyanobacteria but with overall low sequence identity (Table S3). All three LphTPS candidates appear to be single-domain, harboring two conserved Mg^{2+}-cofactor-binding motifs typical of type I sesquiterpene synthases (Figure S3).[3]

While no sesquiterpene synthase from red algae has been previously characterized and deposited in GenBank to date, the transcriptome of another sesquiterpene-producing *Laurencia* species, *Laurencia dendroidea*, is available through the NCBI Sequence Read Archive (SRA).[23] Mining sesquiterpene synthases in the *L. dendroidea* transcriptome identified three red algal sesquiterpene synthase-encoding genes (Figure S4) homologous to LphTPS-A, -B and -C. In order to infer the organismal origin of sesquiterpene synthases identified from red algal transcriptomes, we performed phylogenetic analysis using LphTPSs together with the *L. dendroidea* sesquiterpene synthases and other representative bacterial, fungal, amoebal and plant sesquiterpene synthases (Figure 2 & S5). This analysis revealed that the six red macroalgal sesquiterpene synthases form a well-supported monophyletic clade separate from sesquiterpene synthases from other domains of life (Figure 2). Since the *L. dendroidea* transcriptome was derived from a cultivated alga with minimized microbial contamination, which exhibited similar sesquiterpene chemotypes,[23] we conclude that LphTPS-A, -B and –C and their homologs in *L. dendroidea* are most likely encoded by the red algal genomes instead of symbiont microbial genomes. Future in-depth (meta)genomic analysis of the *L. pacifica* holobiont is necessary to unequivocally verify the source organism of LphTPSs.[9,24]

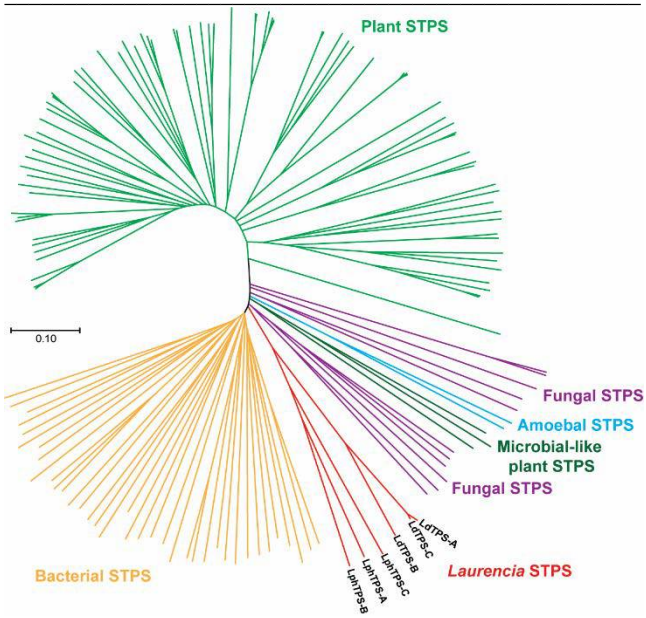

Figure 2. A Neighbor-joining phylogenetic tree including sesquiterpene synthases from transcriptomes of *L. pacifica* and *L. dendroidea* and select bacterial, fungal, amoebal and plant sesquiterpene synthases. The scale measures evolutionary distances in substitutions per amino acid. For detailed tree with complete references bootstrap values, see Figure S5. Abbreviation: STPS, sesquiterpene synthases.

For biochemical identification, we initially chose LphTPS-A for production of its sesquiterpene products in heterologous hosts. LphTPS-A was expressed in the *S. cerevisiae* BY4743 strain using the p426TEF expression vector.[25] After five days of culturing, hexane extracts of the yeast cells were prepared, and analyzed by GC-MS. One major sesquiterpene product and several minor products were detected

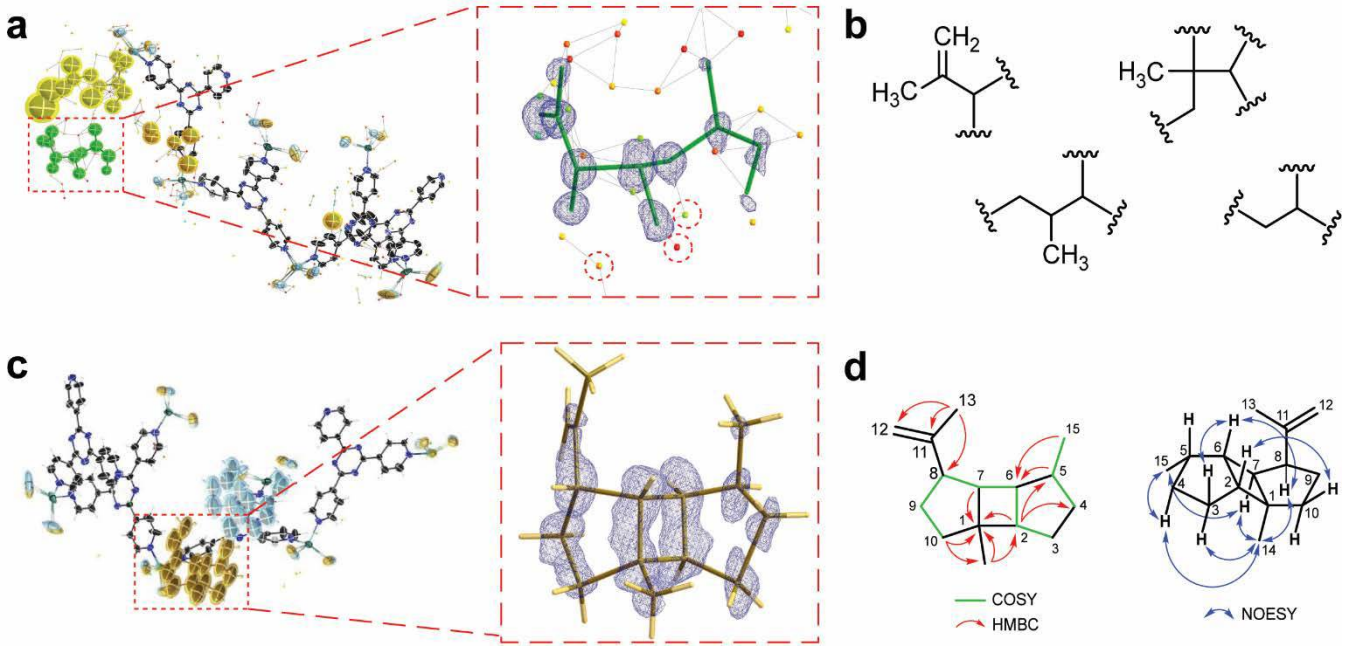

Figure 3. Characterization of LphTPS-A as a prespatane sesquiterpene synthase by microgram-scale NMR-coupled crystalline sponge XRD analysis. (a) The preliminary X-ray diffraction refinement result of the crystalline sponge-**3** complex (Table S7). The zoomed insert shows the partial solution of **3** superimposed with the Fourier electron density map (σ = 0.6, red box). (b) Partial structural motifs of **3** inferred from NMR analysis. (c) The final X-ray diffraction refinement result of the crystalline sponge-**3** complex. Two crystallographically independent molecules of prespatane (**3**) are present in each asymmetric unit (guest **A** - yellow color, guest **B** – blue color). The zoomed insert shows the final structure of prespatane superimposed with the Fourier electron density map (guest **A**, σ = 0.55, red box). (d) NMR confirmation of the prespatane structure. ^{1}H-^{1}H COSY and key HMBC correlations in **3** and key NOESY correlations in **3** are displayed.

(Figure 1c). The main product **3** matched one of the observed major sesquiterpene chemotypes from the *L. pacifica* holobiont based on MS analysis (Figure 1c, Figure S6)**.** Compound **3** was subsequently purified from transgenic yeast cell pellet, and concentrated to oil with sub-milligram yields for structure elucidation.

To resolve the structure of **3**, we used the crystalline sponge method.[14,15,17,26,27,28] Each single crystal of the $[(ZnI_2)_2(tpt)_3 \cdot x(solvent)]_n$ porous complex (crystalline sponge, tpt, tris(4-pyridyl)-1,3,5-triazine)[29] was placed in a vial containing cyclohexane (45 µL), to which a solution of **3** in 1,2-dichloroethane (5 µL, 1 mg/mL) was added. The vial was capped and a syringe needle was inserted on top to allow slow evaporation of the solvent at 50 ˚C for 1 day followed by 5 days at 4 ˚C. The guest-absorbed crystals were subjected to XRD analysis using an in-house X-ray diffractometer using Cu *K*α irradiation. The space group of the crystalline sponge changed from centrosymmetric *C*2/*c* to non-centrosymmetric *C*2 following guest molecule absorption (Figure S7). Initial structure elucidation and refinement resolved a clear C12 moiety with a statistically significant match of the F_o and F_c maps (Figure 3a). This *de novo* partial solution was notably unbiased as neither restraints nor constraints were employed at this initial stage of structure determination (Dataset S1-9, Figure S8, Table S4-7).

Next, NMR spectroscopic analyses were conducted to gain additional chemical information of **3** (Figures S9–S15, Table S8). The molecular formula of **3**, $C_{15}H_{24}$, gives a degree of unsaturation of four, which indicates either a multicyclic structure or a linear molecule with four double bonds. These alternatives were resolved using ^{13}C NMR. The ^{13}C NMR spectrum revealed 15 signals including one terminal olefinic carbon. Given the degree of unsaturation of four and just one double bond in the molecule, **3** conforms to a tricyclic structure. Interpretations of DEPT, HMQC, ^{1}H-^{1}H COSY, and HMBC correlations further suggested the presence of four *de novo* partial structural motifs in **3** as shown in Figure 3b.

Combining the *de novo* partial solutions of **3** from both the initial X-ray interpretation and the NMR data led to definitive assignment of the remaining three carbons missing from the partial *de novo* X-ray solution (Dataset S10-15, Figure S8, Table S8-10). This combined interpretation was further supported by three previously unaccounted peaks of electron density near the C12 moiety (Figure 3b). A 5-4-5 fused ring tricyclic scaffold was obtained following assignment of these final three carbons and the use of DANG and DFIX restraints based on NMR measurements. Refinement of the crystal structure of the crystalline sponge-**3** complex revealed two crystallographically independent guest molecules of **3** per asymmetric unit (Figure 3c). These guest molecules **A** and **B** were refined as described (Supporting text, Figure S8). The following discussion is focused on the well-behaved guest **A**, which is a valid methodology.[15] Finally, DFIX and most DANG restraints were removed during the last stages of refinement against the X-ray data (Dataset S16-20, Figure S8, Table S11-14).

The absolute configuration of the tricyclic C15 structure of **3** was established as 1*S*, 2*R*, 5*S*, 6*S*, 7*S*, 8*S*, based on the Flack parameters [0.057(6)] calculated using the Parsons' method (Table S14, CCDC Entry: 1533929). This configuration was confirmed by unsuccessful matching of its enantiomer structure to the X-ray data (Dataset S21-24, Figure S8, Table S15 & S16). The final structure of **3** was double-checked against the ^{1}H-^{1}H COSY, HMBC and NOESY correlations to be fully compliant (Figure 3d).

The connectivity pattern of the resolved structure of **3** matched prespatane (**4**, Figure 4), a bourbonane sesquiterpene isolated from the sponge *Cymbastela hooperi*[30] and the liverwort *Ptychanthus striatus*.[31] However, the absolute configuration of **3** determined here differs from the previously reported relative configuration of prespatane. In this latter case, the relative configuration at prespatane's C8 stereogenic center is opposite to **3**.[30,31] As the previously reported prespatane structure (**4**) was based on NMR data and shares identical ^{13}C-NMR values with **3** (Table S8), we report here

a revised absolute structure of prespatane based on our XRD data (Figure S15).

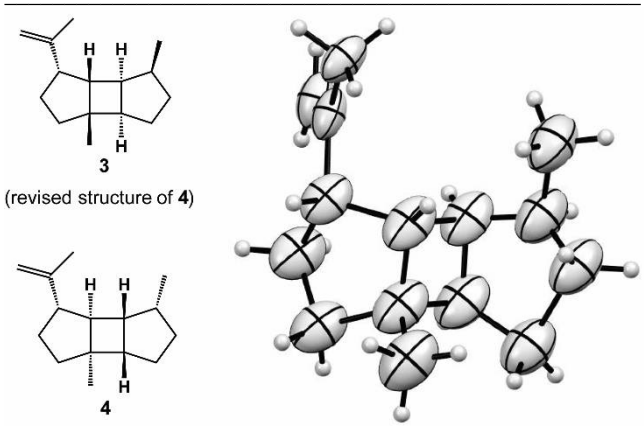

Figure 4. The revised absolute structure of prespatane (**3**) with opposite relative configuration at C8 center compared to the previously reported absolute structure of prespatane (**4**) and ORTEP drawing with 30% probability of guest **A**. [31]

To the best of our knowledge, the absolute structure elucidation of prespatane (**3**) functionally defines LphTPS-A as the first bourbonane-producing sesquiterpene synthase. Bourbonane sesquiterpene natural products feature a 5-4-5 tricyclic scaffold, and have been isolated from numerous plant species, including *Geranium bourbon*,[32] *Vernonia* sp.,[33] and *P. striatus*,[31,34] as well as marine organisms, including the sponge *C. hooperi*,[30] and the soft coral *Nephthea erecta*[35] (Figure S16). The bourbonane ring system is also found in some diterpenes, such as the anti-cancer agent spatol, isolated from the brown macroalga *Spatoglossum schmittii*[36] (Figure S16). In addition, LphTPS-A is the first biochemically characterized sesquiterpene synthase from red macroalgae. Class I sesquiterpene synthases have been hypothesized to be involved in the initial biosynthetic step of red macroalgal halogenated sesquiterpene natural products.[21] The identification of a red macroalgal sesquiterpene synthase and the workflow we applied for its definition will therefore facilitate future investigation of additional sesquiterpene synthases involved in the biosynthesis of therapeutically promising sesquiterpenes from the transcriptomes and genomes of *Laurencia* species.

Prespatane does not appear to be a biosynthetic intermediate of the main sesquiterpenes **1** and **2** in *L. pacifica*. However, vanadium-dependent bromoperoxidases[21] and other sesquiterpene-modifying enzymes may transform prespatane to halogenated natural products such as **1** and **2**. Alternatively, LphTPS-B and LphTPS-C could produce the corresponding sesquiterpene intermediates of **1** and **2**. Studies regarding the potential turnover of prespatane by bromoperoxidases identified from the *L. pacifica* transcriptome and characterization of the other *L. pacifica* sesquiterpene synthases are currently underway.

Prespatane biosynthesis was previously investigated by stable isotope labeling in the liverwort *P. striatus*.[34] Katoh *et al.* established the positions of the (*E,E*)-FPP-derived five carbon isoprene units in the prespatane scaffold by *in vivo* incorporation of [2-^{13}C]-mevalonolactone and [5,5-D_2]-mevalonolactone (Figure S17), which enabled the authors to propose a cyclization mechanism accompanying prespatane biosynthesis.

The establishment of the absolute configuration of prespatane (**3**) and the identification of LphTPS-A as a prespatane synthase determined herein led us to propose refined catalytic mechanisms underpinning prespatane formation by LphTPS-A from (*E,E*)-FPP (Scheme 1). In the first step, (*E,E*)-FPP ionizes through loss of diphosphate, and the resultant farnesyl cation undergoes an initial [1,10]-cyclization to form a germacrenyl cation. In the proposed pathway *a*, germacrene A is formed by C12/C13 deprotonation. Subsequently, reprotonation of germacrene A yields the second cyclization and proton abstraction at C7 initiates the final cyclization step to give prespatane.[34] In the proposed pathway *b*, germacrenyl cation undergoes a deprotonation at C8 to form germacrene B. Germacrene B reprotonation triggers two steps of cyclization and a subsequent rearrangement to yield the final carbocation with a bourbonane scaffold which gets deprotonated to form prespatane. In the proposed pathway c, germacrene C is formed from germacrenyl cation by a 1,2-hydride shift and deprotonation at C7. Reprotonation of germacrene C initiates two consecutive carbocation-mediated cyclization steps leading to the prespatane skeleton. Following a second 1,2-hydride shift and deprotonation of the terminal tertiary carbocation prespatane (**3**) forms. To test these proposed catalytic mechanisms, LphTPS-A was heterologously expressed in *E. coli*, and purified to homogeneity for *in vitro* enzyme assays (Figure S18). Incubation of LphTPS-A with (*E,E*)-FPP and Mg^{2+} yielded prespatane (Figure S18), while incubation with geranyl diphosphate (GPP) or geranylgeranyl diphosphate (GGPP) resulted in no terpene product formation, confirming LphTPS-A as a sesquiterpene synthase specific for 15-carbon substrates. Furthermore, LphTPS-A was incubated with (*E,E*)-FPP and Mg^{2+} in D_2O.[37] The EI-MS spectrum of prespatane formed in D_2O showed a 205 m/z parent mass peak (Figures S18), supporting a deprotonation-reprotonation step during prespatane formation (Scheme 1) due to deuterium incorporation into the prespatane skeleton. Specifically, EI-MS analysis of the deuterated prespatane suggests a reprotonation at C5 instead of C1 as indicated (Figure S18) in comparison to prior prespatane EI-MS fragmentation analyses.[34] A recent study of a fungal guaia-6,10(14)-diene synthase elucidated a single step pathway from germacrene C to the guaianyl cation upon protonation-based activation of germacrene C to initiate cyclization,[38] a feature likely shared with LphTPS-A-mediated catalysis. Ultimately, the discovery of LphTPS-A aids future efforts in resolving the mechanistic bases for bourbonane sesquiterpene biosynthesis in *L. pacifica* and other systems.

Scheme 1. Proposed cyclization mechanisms of prespatane (**3**) from FPP catalyzed by LphTPS-A.

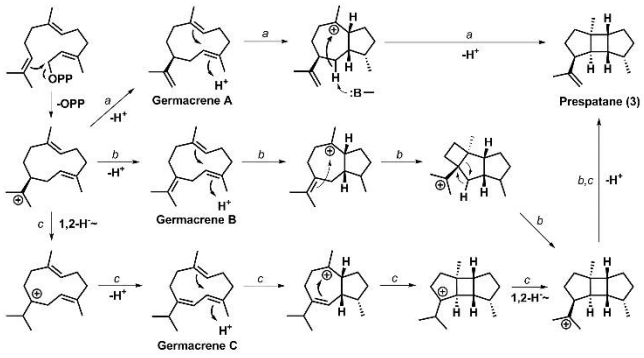

CONCLUSIONS

In summary, we report the discovery of the first bourbonane-producing sesquiterpene synthase from red macroalga *L. pacifica* by the combination of metabolomics, transcriptomics, metabolic engineering in yeast, and microgram-scale NMR-coupled crystalline sponge XRD analysis. We showed that red macroalgae can

produce sesquiterpenes via class I sesquiterpene synthases and that these marine organisms can be a source of new terpene chemistry and biochemistry. This study demonstrated that the absolute structure elucidation of sesquiterpene natural products from microgram-scale quantities could be efficiently achieved by combining information yielded from both NMR analyses and the crystalline sponge method. The structural revision of prespatane also marks the first application of the crystalline sponge method for *de novo* structure elucidation of an unknown analyte with NMR complementation in an iterative fashion. Future studies will focus on systematic analysis of functionally diverse sesquiterpene synthases to assess general applicability of this newly established workflow. Further methodology improvements of the crystalline sponge technique regarding sample preparation and data analysis could make it an important part for the routine structure-function characterization of terpene biosynthetic enzymes and, therefore, expedite the discovery of largely unexplored terpene chemistry and biochemistry in source-limited non-model organisms.

ASSOCIATED CONTENT

Supporting Information

The Supporting Information is available free of charge on the ACS Publications website.
Full experimental procedures and characterization data (pdf).

Accession Codes

RNA transcripts identified in this study have been deposited into NCBI GenBank under the following accession numbers: LphTPS-A (KY689932), LphTPS-B (KY689933), and LphTPS-C (KY689934). Raw RNA-Seq reads have been submitted to NCBI SRA (SRR5314125, SRR5314126). The *de novo* transcriptome used in this study has been submitted to NCBI TSA (xxxxx). A vector containing codon-opimized *LphTPS-A* has been deposited to Addgene (89468). The crystallographic data described in this paper has been deposited to the Cambridge Crystallographic Data Centre (1533929). LC-MS/MS spectra of laurinterol, pacifenol and prespatane have been deposited to the GNPS spectral library.[39]

AUTHOR INFORMATION

Corresponding Author

mfujita@appchem.t.u-tokyo.ac.jp and wengj@wi.mit.edu

Notes

J.K.W. is a co-founder, a member of the Scientific Advisory Board, and a shareholder of DoubleRainbow Biosciences, Inc., which develops biotechnologies related to natural products.

ACKNOWLEDGMENT

We thank Peter Müller for critically reviewing the XRD data analysis, and Gerald Fink for kindly providing the yeast strain *S. cerevisiae* BY4743 and the yeast protein expression vector p426TEF. J.P.N. is an investigator with the Howard Hughes Medical Institute and holds the Arthur and Julie Woodrow Chair at the Salk Institute. R.D.K. is a Howard Hughes Medical Institute postdoctoral fellow of the Life Sciences Research Foundation. T.P. is a Simons Foundation postdoctoral fellow of the Helen Hay Whitney Foundation. This work was supported by the Pew Scholar Program in the Biomedical Sciences (J.K.W.), the Searle Scholars Program (J.K.W.), and the JST-ACCEL program (M. F.).

REFERENCES

1. Breitmaier, E. Terpenes: Flavors, Fragrances, Pharmaca, Pheromones, Wiley-VCH, Weinheim, Germany, **2006**.
2. Gershenzon, J.; Dudareva, N. *Nat. Chem. Biol.* **2007**, *3*, 408−414.
3. Gao, Y.; Honzatko, R. B.; Peters, R. J. *Nat. Prod. Rep.* **2012**, *29*, 1153−1175.
4. Maimone, T. J.; Baran, P. S. *Nat. Chem. Biol.*, **2007**, *3*, 396-407.
5. Ro, D. K.; Paradise, E. M.; Ouellet, M.; Fisher, K. J.; Newman, K. L.; Ndungu, J. M.; Ho, K. A.; Eachus, R. A.; Ham, T. S.; Kirby, J.; Chang, M. C. *Nature* **2006**, *440*, 940-943.
6. Yamada, Y.; Kuzuyama, T.; Komatsu, M.; Shin-ya, K.; Omura, S.; Cane, D. E.; Ikeda, H. *Proc. Nat. Acad. Sci. U.S.A.* **2015**, *112*, E857-862.
7. Quin, M. B.; Flynn, C. M.; Schmidt-Dannert, C. *Nat. Prod. Rep.* **2014**, *31*, 1449-1473.
8. Boutanaev, A. M.; Moses, T.; Zi, J.; Nelson, D. R.; Mugford, S. T.; Peters, R. J., Osbourn, A. *Proc. Nat. Acad. Sci. U.S.A.* **2015**, *112*, E81-E88.
9. Chen, X.; Köllner, T. G.; Jia, Q.; Norris, A.; Santhanam, B.; Rabe, P.; Dickschat, J. S.; Shaulsky, G.; Gershenzon, J.; Chen, F. *Proc. Nat. Acad. Sci. U.S.A.* **2016**, *113*, E12132-12137.
10. Chow, J. Y.; Tian, B. X.; Ramamoorthy, G.; Hillerich, B. S.; Seidel, R. D.; Almo, S. C.; Jacobson, M. P.; Poulter, C. D. *Proc. Nat. Acad. Sci. U.S.A.* **2015**, *112*, E5661-5666.
11. Rodriguez, S.; Kirby, J.; Denby, C. M.; Keasling, J. D. *Nat. Prot.* **2014**, *9*, 1980-1996.
12. Torrens-Spence, M.P.; Fallon, T.R.; Weng, J.K. *Methods Enzymol.* **2016**, *576*, 69-97.
13. Rabe, P.; Dickschat, J. S. *Angew. Chem., Int. Ed.* **2013**, 52, 1810-1812.
14. Inokuma, Y.; Yoshioka, S.; Ariyoshi, J.; Arai, T.; Hitora, Y.; Takada, K.; Matsunaga, S.; Rissanen, K.; Fujita, M. *Nature* **2013**, *495*, 461-466. Corrigendum: *Nature* **2013**, *501*, 262.
15. Hoshino, M.; Khutia, A.; Xing, H.; Inokuma, Y.; Fujita, M. 2016. *IUCrJ* **2016**, *3*, 139-151.
16. Zigon, N.; Hoshino, M.; Yoshioka, S.; Inokuma, Y.; Fujita, M. *Angew. Chem., Int. Ed.* **2015**, *127*, 9161-9165.
17. Lee, S.; Kapustin, E. A.; Yaghi, O. M. *Science* **2016**, *353*, 808-811.
18. Matsuda, Y.; Mitsuhashi, T.; Lee, S.; Hoshino, M.; Mori, T.; Okada, M.; Zhang, H.; Hayashi, F.; Fujita, M.; Abe, I. *Angew. Chem., Int. Ed.* **2016**, *128*, 5879-5882.
19. Urban, S.; Brkljača, R.; Hoshino, M.; Lee, S.; Fujita, M. *Angew. Chem., Int. Ed.* **2016**, *55*, 2678-2682.
20. Wang, B. G.; Gloer, J. B.; Ji, N. Y.; Zhao, J. C. *Chem. Rev.* **2013**, *113*, 3632-3685.
21. Butler, A.; Carter-Franklin, J. N. *Nat. Prod. Rep.* **2004**, *21*, 180-188.
22. Sims, J. J.; Fenical, W.; Wing, R. M.; Radlick, P. *J. Am. Chem. Soc.* **1971**, *93*, 3774-3775.
23. de Oliveira, L.S.; Tschoeke, D.A.; de Oliveira, A.S.; Hill, L.J.; Paradas, W.C.; Salgado, L.T.; Thompson, C.C.; Pereira, R.C.; Thompson, F.L. *Mar. Drugs* **2015**, 13, 879-902.
24. Agarwal, V.; Blanton, J.M.; Podell, S.; Taton, A.; Schorn, M.A.; Busch, J.; Lin, Z.; Schmidt, E.W.; Jensen, P.R.; Paul, V.J.; Biggs, J.S. *Nat. Chem. Biol.* **2017**, *13*, 537-543.
25. Mumberg, D.; Müller, R.; Funk, M. *Gene* **1995**, *156*, 119-122.
26. Ramadhar, T. R.; Zheng, S.; Chen, Y.; Clardy, J. *Acta Crystallogr. Sect. A* **2015**, *71*, 46-58.
27. Hayes, L. M.; Knapp, C. E.; Nathoo, K. Y.; Press, N. J.; Tocher, D. A.; Carmalt, C. *J. Cryst. Growth Des.* **2016**, *16*, 3465-3472.
28. Lee, S.; Hoshino, M.; Fujita, M.; Urban, S. *Chem. Sci.* **2017**, *8*, 1547-1550.
29. Biradha, K.; Fujita, M. *Angew. Chem. Int. Ed.* **2002**, *41*, 3392-3395.
30. König, G. M.; Wright, A. D. *J. Org. Chem.* **1997**, *62*, 3837-3840.
31. Nabeta, K.; Yamamoto, M.; Koshino, H.; Fukui, H.; Fukushi, Y.; Tahara, S. *Biosci., Biotechnol. Biochem.* **1999**, *63*, 1772 1776.
32. Křepinský, J.; Samek, Z.; Šorm, F.; Lamparsky, D.; Naves, Y. R. *Tetrahedron* **1966**, *22*, 53-70.
33. Bohlmann, F.; Jakupovic, J.; Gupta, R. K.; King, R. M.; Robinson, H. *Phytochemistry*, **1981**, *20*, 473-480.

34. Nabeta, K.; Yamamoto, M.; Fukushima, K.; Katoh, K. *Perkin Trans. 1*, **2000**, *16*, 2703-2708.
35. Cheng, S. Y.; Dai, C. F.; Duh, C. Y. *J. Nat. Prod.* **2007**, *70*, 1449-1453.
36. Gerwick, W. H.; Fenical, W.; Van Engen, D.; Clardy, J. *J. Am. Chem. Soc.* **1980**, *102*, 7991-7993.
37. Jiang, J.; He, X.; Cane, D. E. *J. Am. Chem. Soc.* **2006**, *128*, 8128-8129.
38. Burkhardt, I.; Siemon, T.; Henrot, M.; Studt, L.; Rösler, S.; Tudzynski, B.; Christmann, M.; Dickschat, J. S. *Angew. Chem., Int. Ed.* **2016**, *55*, 8748-8751.
39. Wang, M.; Carver, J.J.; Phelan, V.V.; Sanchez, L.M.; Garg, N.; Peng, Y.; Nguyen, D.D.; Watrous, J.; Kapono, C.A.; Luzzatto-Knaan, T.; Porto, C.; Bouslimani, A.; Melnik, A.V.; Meehan, M.J.; Liu, W.T.; Crüsemann, M.; Boudreau, P.D.; Esquenazi, E.; Sandoval-Calderón, M.; Kersten, R.D.; Pace, L.A.; Quinn, R.A.; Duncan, K.R.; Hsu, C.C.; Floros, D.J.; Gavilan, R.G.; Kleigrewe, K.; Northen, T.; Dutton, R.J.; Parrot, D.; Carlson, E.E.; Aigle, B.; Michelsen, C.F.; Jelsbak, L.; Sohlenkamp, C.; Pevzner, P.; Edlund, A.; McLean, J.; Piel, J.; Murphy, B.T.; Gerwick, L.; Liaw, C.C.; Yang, Y.L.; Humpf, H.U.; Maansson, M.; Keyzers, R.A.; Sims, A.C.; Johnson, A.R.; Sidebottom, A.M.; Sedio, B.E.; Klitgaard, A.; Larson, C.B., P, C.A.B.; Torres-Mendoza, D.; Gonzalez, D.J.; Silva, D.B.; Marques, L.M.; Demarque, D.P.; Pociute, E.; O'Neill, E.C.; Briand, E.; Helfrich, E.J.N.; Granatosky, E.A.; Glukhov, E.; Ryffel, F.; Houson, H.; Mohimani, H.; Kharbush, J.J.; Zeng, Y.; Vorholt, J.A.; Kurita, K.L.; Charusanti, P.; McPhail, K.L.; Nielsen, K.F.; Vuong, L.; Elfeki, M.; Traxler, M.F.; Engene, N.; Koyama, N.; Vining, O.B.; Baric, R.; Silva, R.R.; Mascuch, S.J.; Tomasi, S.; Jenkins, S.; Macherla, V.; Hoffman, T., Agarwal, V.; Williams, P.G.; Dai, J.; Neupane, R.; Gurr, J.; Rodríguez, A.M.C.; Lamsa, A.; Zhang, C.; Dorrestein, K.; Duggan, B.M.; Almaliti, J.; Allard, P.M.; Phapale, P.; Nothias, L.F.; Alexandrov, T.; Litaudon, M.; Wolfender, J.L.; Kyle, J.E.; Metz, T.O.; Peryea, T.; Nguyen, D.T.; VanLeer, D.; Shinn, P.; Jadhav, A.; Müller, R.; Waters, K.M.; Shi, W.; Liu, X.; Zhang, L.; Knight, R.; Jensen, P.R.; Palsson, B.O.; Pogliano, K.; Linington, R.G.; Gutiérrez, M.; Lopes, N.P.; Gerwick, W.H.; Moore, B.S.; Dorrestein, P.C.; Bandeira, N. *Nat. Biotechnol.* **2016**, *34*, 828-837.

TOC graphic

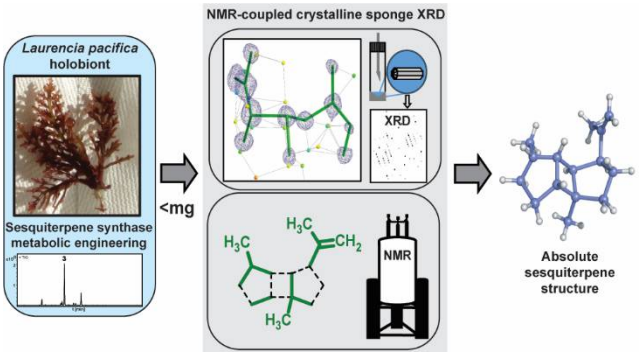
Laurencia pacifica
holobiont
Sesquiterpene synthase
metabolic engineering
<mg
NMR-coupled crystalline sponge XRD
XRD
NMR
Absolute
sesquiterpene
structure

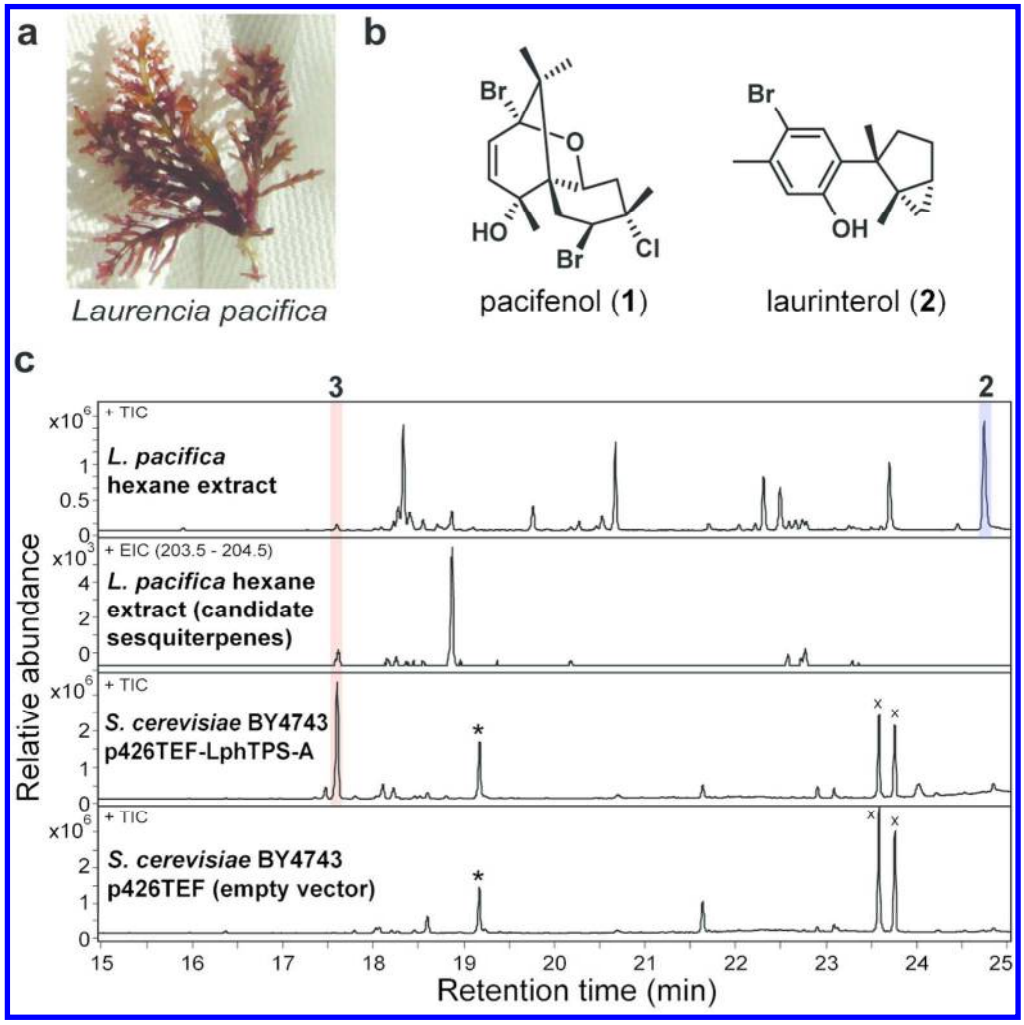

Figure 1. Terpene chemotyping of Laurencia pacifica and expression of LphTPS-A in yeast. (a) L. pacifica specimen. (b) Pacifenol (1) and laurinterol (2). (c) GC-MS detection of a candidate sesquiterpene (3) in L. pacifica hexane extract and reconstitution of the production of 3 in yeast by recombinant expression of LphTPS-A. The red bar highlights sesquiterpene 3, the blue bar highlights laurinterol (2). Asterisk denotes (E,E)-farnesol and x denotes fatty acids based on NIST EI-MS match.

104x104mm (300 x 300 DPI)

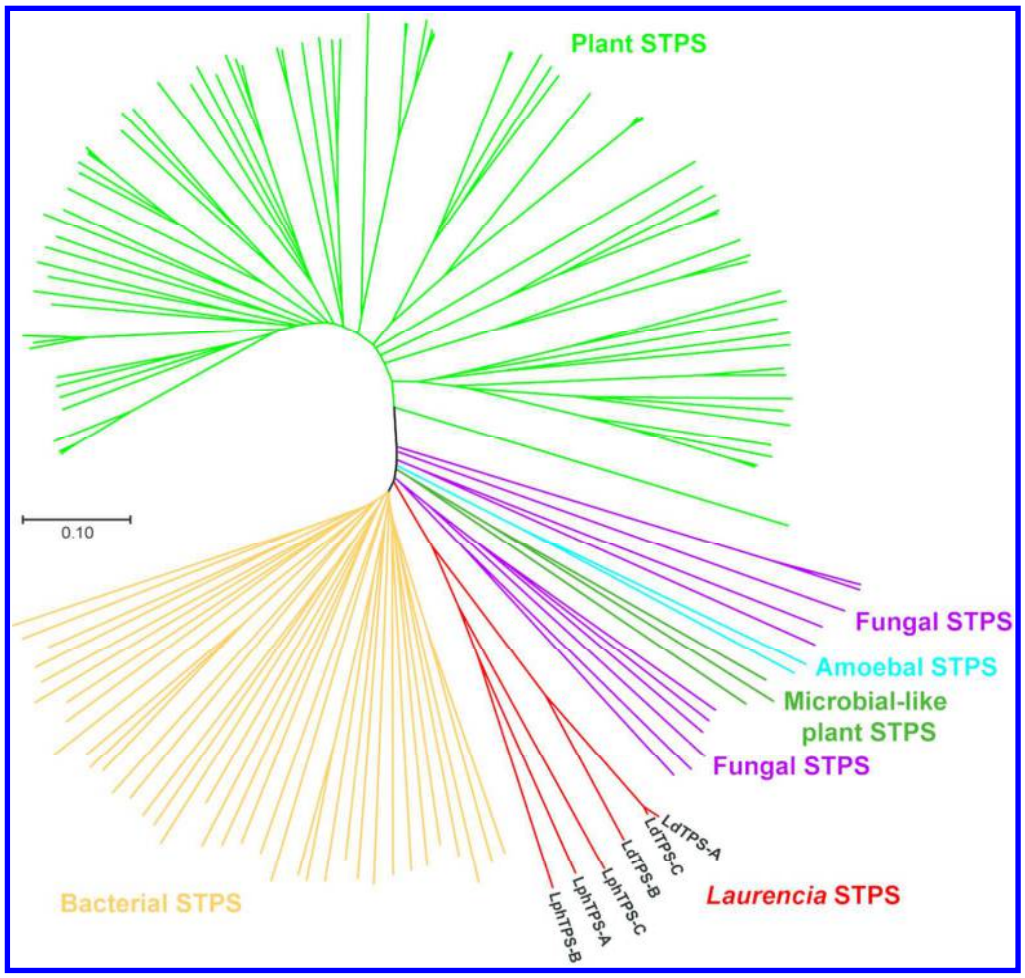

Figure 2. A Neighbor-joining phylogenetic tree including STPSs from transcriptomes of L. pacifica and L. dendroidea and select bacterial, fungal, amoebal and plant STPSs. The scale measures evolutionary distances in substitutions per amino acid. For de-tailed tree with complete references bootstrap values, see Figure S5. Abbreviation: STPS, sesquiterpene synthases.

110x104mm (300 x 300 DPI)

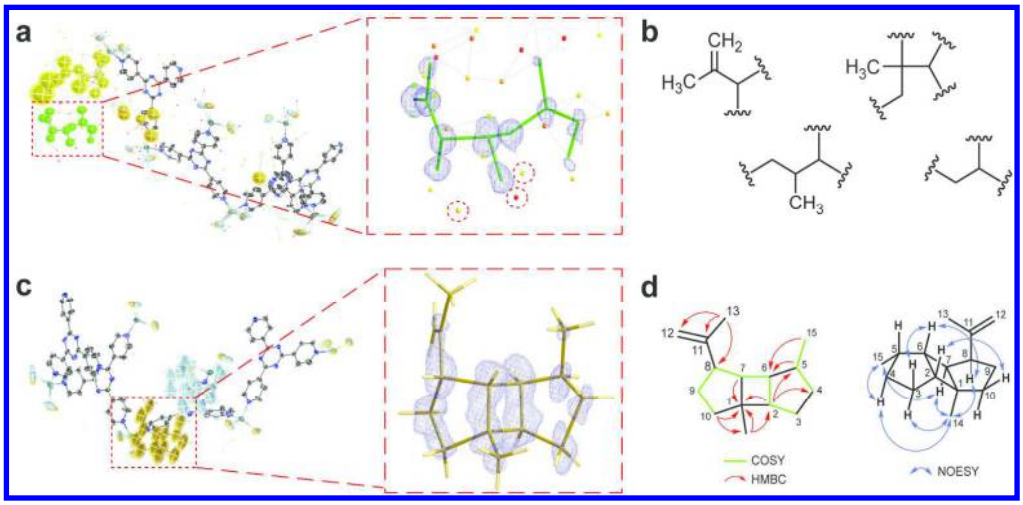

Figure 3. Characterization of LphTPS-A as a prespatane STPS by microgram-scale NMR-coupled crystalline sponge XRD analysis. (a) The preliminary X-ray diffraction refinement result of the crystalline sponge-3 complex (Table S7). The zoomed insert shows the partial solution of 3 superimposed with the Fourier electron density map (σ = 0.6, red box). (b) Partial structural motifs of 3 inferred from NMR analysis. (c) The final X-ray diffraction refinement result of the crystalline sponge-3 complex. Two crystallographically independent molecules of prespatane (3) are present in each asymmetric unit (guest A - yellow color, guest B – blue color). The zoomed insert shows the final structure of prespatane superimposed with the Fourier electron density map (guest A, σ = 0.55, red box). (d) NMR confirmation of the prespatane structure. 1H-1H COSY and key HMBC correlations in 3 and key NOESY correlations in 3 are displayed.

209x100mm (300 x 300 DPI)

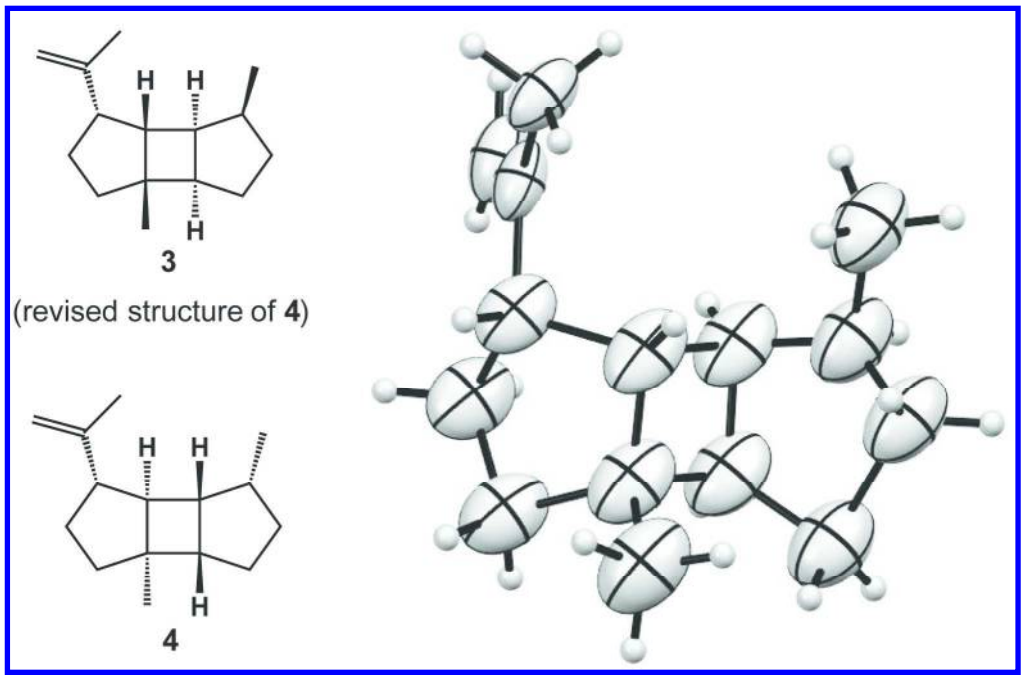

Figure 4. The revised absolute structure of prespatane (3) with opposite relative configuration at C8 center compared to the previously reported absolute structure of prespatane (4) and ORTEP drawing with 30% probability of guest A. 31

184x120mm (300 x 300 DPI)

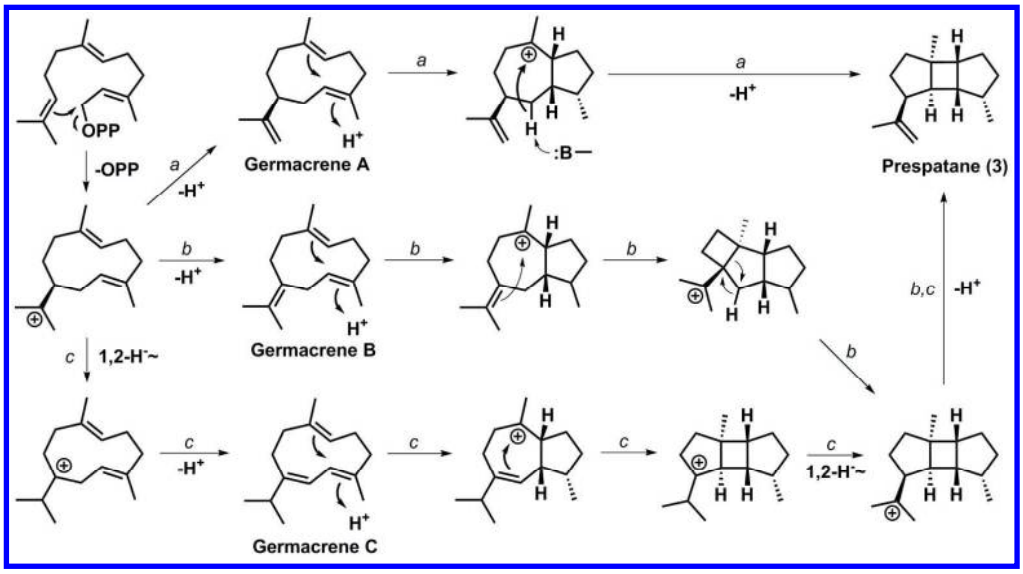

Scheme 1. Proposed cyclization mechanisms of prespatane (3) from FPP catalyzed by LphTPS-A.

192x105mm (300 x 300 DPI)